6

Response of Continuous Pipelines to Longitudinal PGD

As mentioned previously, PGD can be decomposed into longitudinal and transverse components. This chapter discusses the response of continuous pipeline subject to longitudinal PGD (soil movement parallel to the pipe axis). Subsequent chapters will cover the response of continuous pipeline to transverse PGD (soil movement perpendicular to the pipe axis) as well as the response of segmented pipe to PGD.

Under longitudinal PGD, a corrosion-free continuous pipeline may fail at welded joints, may buckle locally (wrinkle) in a compressive zone, and/or may rupture in a tensile zone. When the burial depth is very shallow, the pipeline may buckle like a beam in a ground compressive zone as discussed in Chapter 4.

Two separate models of buried pipe response to longitudinal PGD are presented herein. In the first model, the pipeline is assumed to be linear elastic. This model is often appropriate for buried pipe with slip joints since, as shown in Chapter 4, slip joints typically fail at load levels for which the rest of the pipe is linear elastic. In the second model, the pipeline is assumed to follow a Ramberg Osgood type stress-strain relation as given in Equation 4.1. This model is often appropriate for pipe with arc welded butt joints, since the local buckling or tensile rupture failure modes typically occur when the pipe is beyond the linear elastic range. Conditions leading to local buckling failure are presented, as well as those for tensile rupture. Finally the effect of flexible expansion joints are discussed. For each of these situations, case history comparisons are presented when available.

6.1

ELASTIC PIPE MODEL

As noted previously, the pattern of ground deformation has an effect upon the response of continuous pipelines to longitudinal PGD. Examples of observed longitudinal patterns were presented in Figure 2 10. For the purpose of analysis, M. O'Rourke and Nordberg (1992) have idealized five patterns as shown in Figure 6.1. That is, the Block pattern in Figure 6 1(a) is an idealization of the relatively uniform longitudinal pattern in Figure 2 10(a) (Section Line N-2) while the Ramp, Ramp-Block, Symmetric Ridge and Asymmetric Ridge pattern are idealization of the observed patterns in Figure 2-10 (b), (c), (d) and (e) respectively.

Assuming elastic pipe material and using either elasto-plastic or rigid-plastic force-deformation relations at the soil-pipe interface, M. O'Rourke and Nordberg (1992) analyzed the response of buried steel pipeline to three idealized patterns of longitudinal PGD (i.e., Ramp, Block and Symmetric Ridge).

Due to the small values for x_u, the maximum elastic deformation for the longitudinal "soil springs" discussed in Chapter 5, they found that the response for a simplified rigid-plastic model of the soil-pipe interaction gives essentially the same results as a more complex elasto-plastic model for the soil-pipe interface The maximum pipe strain, ε, for all three patterns, normalized by the equivalent ground strain , is plotted as a function of the normalized length of the PGD zone in Figure 6.2. The length of the PGD zone is normalized by the embedment length, L_{em}, which is defined as the length over which the constant slippage force t_u must act to induce a pipe strain equal to the equivalent ground strain. Note that the Block pattern results in the largest strain in an elastic pipe.

For the Block pattern of PGD, the strain in an elastic pipe is then given by:

$$\varepsilon = \begin{cases} \dfrac{\alpha L}{2L_{em}} & L < 4L_{em} \\ \dfrac{\alpha L}{\sqrt{4L_{em}}} & L > 4L_{em} \end{cases} \qquad (6.1)$$

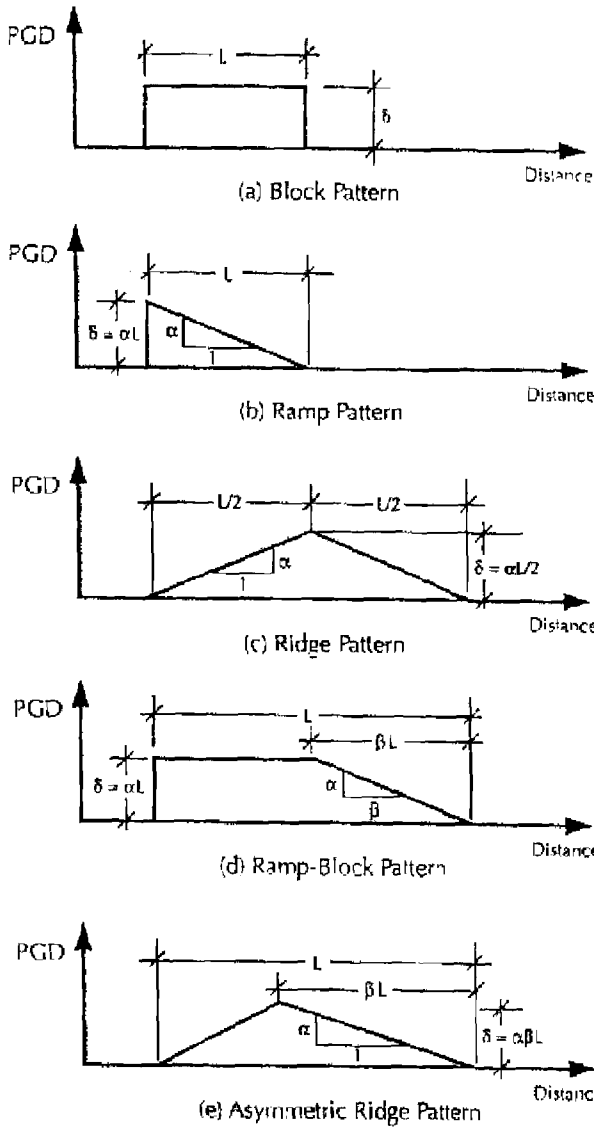

M. O'Rourke et al., 1995

■ Figure 5.1 Five Idealization Patterns

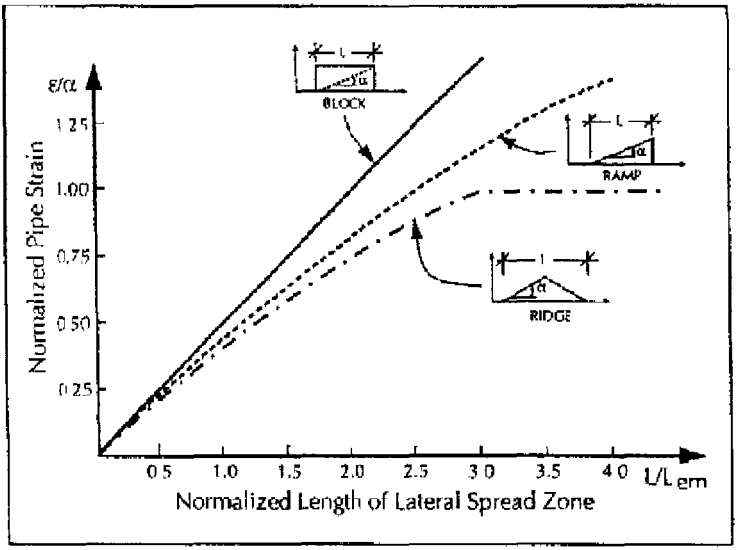

After M. O'Rourke and Nordberg, 1992

■ Figure 6.2 Normalized Pipe Strain as Function of Normalized Length of the Lateral Spread Zone for Three Idealized Patterns of PGD

$$L_{em} = \frac{\alpha EA}{t_u} \tag{6.2}$$

Flores-Berrones and M. O'Rourke (1992) extended the model for a linear elastic pipe with a rigid-plastic "soil spring" (i.e., maximum resistance t_u for any non-zero relative displacement at the soil pipe interface) to the Ramp Block and Asymmetric Ridge patterns. They assigned the most appropriate of the five idealized patterns in Figure 6.1 to each of the 27 observed patterns presented by Hamada et al (1986) and determined the peak pipe strain. They found that the idealized block pattern (that is Equation 6.1) gave a reasonable estimate of pipe response for all 27 of the observed patterns. This is shown in Figure 6.3 wherein the calculated maximum strain in two elastic pipes ϕ=27°, H=0.9 m (3 ft), t=1.9 cm (3/4 in) for Pipe 1 and ϕ=35°, H=1.8 m (6 ft), t=1.27 cm (1/2 in) for Pipe 2) with the appropriate idealized PGD pattern are plotted against the value from Equations 6.1 (i.e., an assumed Block pattern).

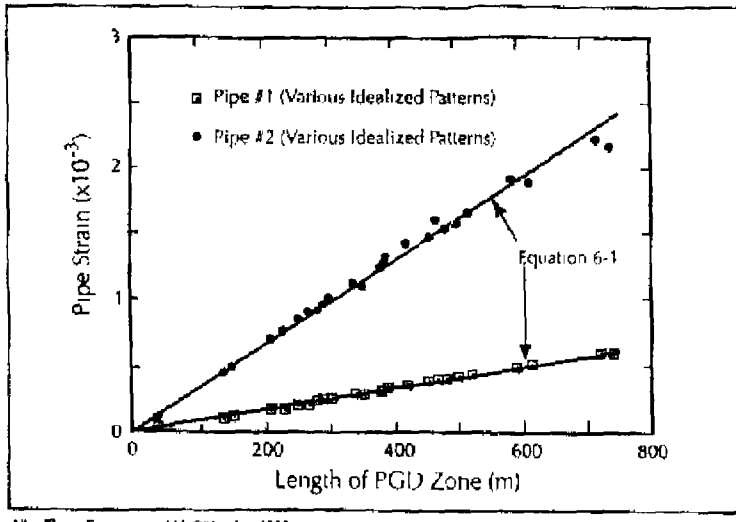

After Flores-Berrones and M. O'Rourke, 1992

■ Figure 6.3 Maximum Strain in Two Elastic Pipes

Some of the pipeline damage in the 1994 Northridge earthquake provide case histories for comparison with the elastic pipe model. Three out of seven pipelines along Balboa Blvd. were damaged due to the longitudinal PGD. Figure 6 4 shows a map of the PGD zone and the locations of the pipe breaks on Balboa Blvd.,

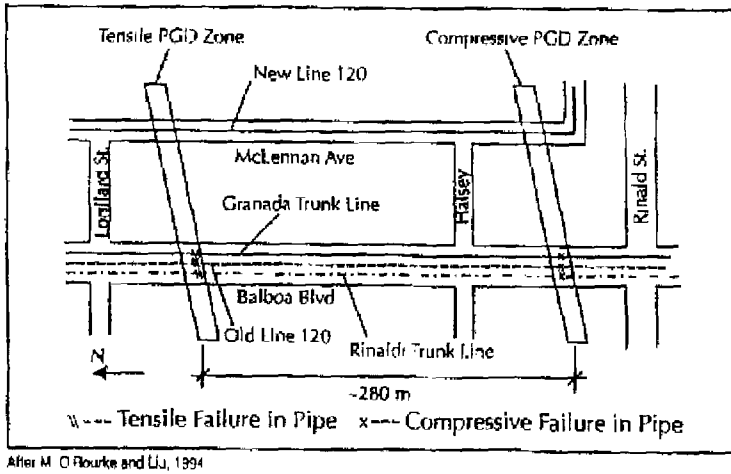

After M. O'Rourke and Liu, 1994

■ Figure 6.4 Map of Ground Deformation Zones and Locations of Pipeline Damage on Balboa Blvd.

in which the two parallelograms are the margins of the PGD zone. According to T. O'Rourke and M. O'Rourke (1995), the length or spatial extent of the PGD zone along Balboa Blvd. was 280 m (918 ft) and the amount of movement was about 0.50 m (20 in).

The properties of those three damaged pipelines are shown in Table 6.1. Note that all these pipelines are made of Grade-B steel.

■ Table 6.1 Properties of Three Damaged Pipelines

Pipeline	Diameter (mm)	Thickness (mm)	σ_y (MPa)	Burial Depth (m)	Coating	Joints
Chinada Trunk Line	1260	6.4	249	1.8	Cement Mortar	Slip joints
Rinaldi Trunk Line	1730	9.5	249	2.7	Cement Mortar	Slip joints
Oil Line 120	560	7.1	242	1.5	Coal Tar Epoxy	Unshielded Arc Welded

Due to the relatively low strength of slip joints and unshielded arc welded joints, the linear elastic pipeline model discussed above can be used to analyze the behavior of these pipelines.

The interaction force at the pipe-soil interface is evaluated using Equation 5.1, and assuming ϕ=37° for dense sand, k=0.87 for coal tar epoxy, k=1.0 for cement mortar coating and $\bar{\gamma} = 1.88 \times 10^4$ N/m^3 (115 pcf). For the two water trunk lines, the joint efficiency of 0.40 is assumed based upon Figure 4.9. For unshielded arc welded Line-120, the yield strain of the pipe steel is conservatively used as critical strain since the compressive and tensile strength of this type of joints are less than those determined from the yield strength of the pipe steel (T. O'Rourke and M. O'Rourke, 1995). Table 6.2 shows the critical strain for the pipes (i.e., failure condition based on joint efficiency, etc.) as well as the induced seismic strain calculated from Equation 6.1. Since the seismic strain is larger than the critical strain, failure is predicted for each of these pipes, which, as mentioned previously, was the observed behavior.

■ Table 6.2 Computation for Three Damaged Pipelines Along Balboa Blvd.

Pipeline	k	Frictional Coefficient	Joint Efficiency	Critical Strain	L_{cr} (m)	Seismic Strain	Predicted Behavior
Granada Trunk Line	1.0	0.75	0.40	0.48×10^{-3}	50.0	2.1×10^{-3}	Failure
Rinaldi Trunk Line	1.0	0.75	0.40	0.48×10^{-3}	51.0	2.1×10^{-3}	Failure
Old Line 120	0.87	0.63	1.0	1.2×10^{-3}	78.7	1.59×10^{-3}	Failure

6.2 Inelastic Pipe Model

As mentioned previously, local buckling of a pipeline with typical burial depths and arc-welded joints requires a model in which the pipe material is inelastic. Since the Block pattern appears to be the most appropriate model for elastic pipes, M. O'Rourke et al. (1995) assumed a Block pattern for determination of the circumstances leading to local buckling failure due to longitudinal PGD in a pipe with a more realistic Ramberg Osgood material model. The idealized Block pattern, shown in Figure 6.1(a), corresponds to a mass of soil having length L, moving down a slight incline. The soil displacement on either side of the PGD zone is zero, while the soil displacement within the zone is a constant value δ.

Two cases for a buried pipeline subject to a Block pattern of longitudinal PGD were considered. In Case I, the amount of ground movement, δ, is large and the pipe strain is controlled by the length, L, of the PGD zone. In Case II, L is large and the pipe strain is controlled by δ.

The distribution of pipe axial displacement, force and strain are shown in Figure 6.5 for Case I and in Figure 6.6 for Case II. Note that t_u is the friction force per unit length at the pipe-soil interface and L_e is the effective length over which t_u acts.

As shown in Figures 6.5 and 6.6, the force in the pipe over the segment AB is linearly proportional to the distance from Point A.

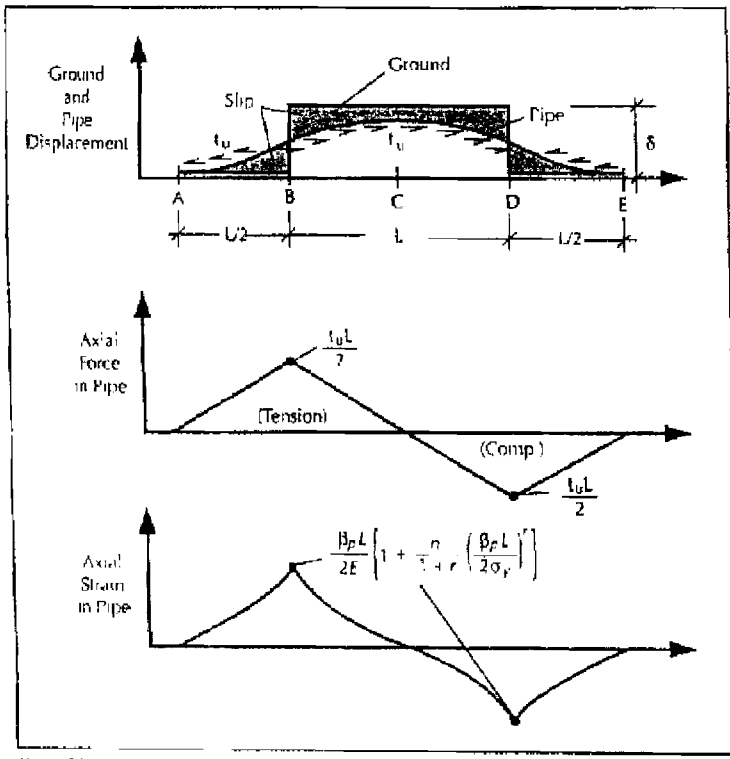

After M. O'Rourke et al., 1995

■ **Figure 6.5 Distribution of Pipe Axial Displacement, Force and Strain for Case I**

Using a Ramberg Osgood model, the pipe strain and displacement can be expressed as follows:

$$\varepsilon(x) = \frac{\beta_p x}{E}\left\{1+\frac{n}{1+r}\left(\frac{\beta_p x}{\sigma_y}\right)^r\right\} \tag{6.3}$$

$$\delta(x) = \frac{\beta_p x^2}{E}\left\{1+\frac{2}{2+r}\cdot\frac{n}{1+r}\cdot\left(\frac{\beta_p x}{\sigma_y}\right)^r\right\} \tag{6.4}$$

where n and r are Ramberg Osgood parameters discussed in Chapter 4, E is the modulus of elasticity of steel, σ_y is the effective yield stress and β_p is the pipe burial parameter, having units of pounds per cubic inch, defined below.

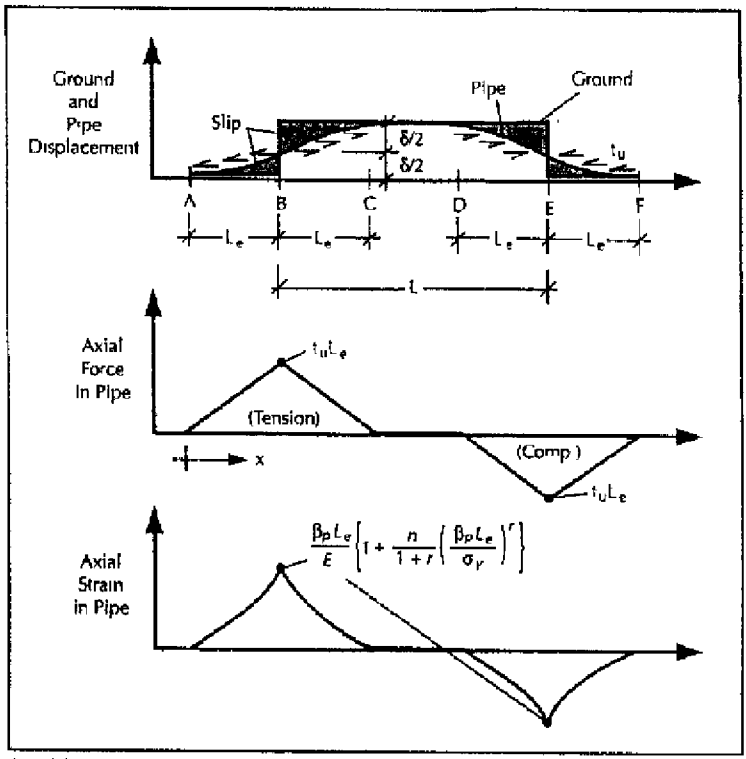

After M. O'Rourke et al., 1995

Figure 6.6 Distribution of Pipe Axial Displacement, Force and Strain for Case II

For sandy soil (c=0), the pipe burial parameter β_p is defined as:

$$\beta_p = \frac{\mu \gamma H}{t} \tag{6.5}$$

where the frictional coefficient μ can be computed by:

$$\mu = \tan k\phi \tag{6.6}$$

For clay, the pipe burial parameter β_p can be expressed as:

$$\beta_p = \frac{\alpha S_u}{t} \tag{6.7}$$

Critical displacement and spatial extent of the PGD zone can be determined by the equations discussed above. Substituting the critical local buckling strain into Equation 6.3, one can obtain the critical length of PGD zone L_c. This can then be used to calculate the critical ground movement δ_c from Equation 6.4. Using the Ramberg Osgood pipe material model, M. O'Rourke et al. (1995) develop critical values for δ and L which result in wrinkling of the pipe wall in compression (critical strain in compression taken as midpoint of range given in Equation 4.3). Table 6.3 shows these critical values for Grade-B (n=10, r=100) and X-70 (n=5.5, r=15.6) steel and a variety of burial parameters and R/t ratios (radius of pipe/thickness).

■ **Table 6.3 Critical Length and Displacement for Compressive Failure of Grade-B and X-70 Steel and Various Burial Parameters and R/t Ratios**

		β_p = 1.0 pci		β_p = 2.5 pci		β_p = 5 pci		β_p = 15 pci		β_p = 25 pci	
	R/t	L(m)	δ(m)	L(m)	δ(m)	L(m)	δ(m)	L(m)	δ(m)	L(m)	δ(m)
GR-B	10	1762	1.32	704	0.53	352	0.26	117	0.09	70	0.05
	25	1744	1.12	698	0.45	349	0.23	116	0.08	70	0.045
	50	1728	1.05	691	0.42	346	0.21	115	0.07	69	0.042
	100	1704	1.00	682	0.4	341	0.20	114	0.066	68	0.04
	150	1660	0.94	664	0.38	332	0.19	111	0.063	66	0.037
X-70	10	4488	10.3	1795	4.1	898	2.10	299	0.69	180	0.41
	25	4182	6.87	1673	2.75	836	1.37	279	0.46	167	0.28
	50	3833	5.18	1533	2.1	768	1.04	256	0.35	153	0.21
	100	2527	2.25	1031	0.90	515	0.45	172	0.15	103	0.09
	150	1718	1.0	687	0.4	344	0.2	115	0.067	69	0.04

A pipe fails in local buckling when both the length and displacement of the PGD zone are larger than the critical values given, for example, in Table 6.3.

As a case history, two X-52 grade steel pipelines (Line 3000 and Mobil Oil) with arc welded joints subject to the longitudinal

PGD at Balboa Blvd. during the 1994 Northridge earthquake are studied here. These two pipelines are a 0.76 m diameter (30 in) gas pipeline and a 0.41 m diameter (16 in) oil pipeline, as listed in Table 6.4.

■ **Table 6.4 Computation for Three Undamaged Pipelines Along Balboa Blvd.**

Pipeline	D (m)	t (mm)	β_p (pci)	Compression		Tension	
				L_{cr} (m)	δ_{cr} (m)	L_{cr} (m)	δ_{cr} (m)
Line 3000	0.76	9.5	10	281	0.11	162	1.57
Mobil Oil	0.41	9.5	4	616	1.25	960	4.2

Based on the ASCE Guidelines (1984), the friction reduction factor is taken as 0.6 for a pipe with epoxy or polyethylene coatings. The corresponding burial parameter is 10 pci (0.28 kgf/cm^3) for the gas line and 4 pci (0.11 kgf/cm^3) for the Mobil line. The critical displacement δ_{cr} and the critical length L_{cr} for both wrinkling and tensile rupture were determined and listed in Table 6.4. For tensile rupture, the critical strain was taken as 4%. Since the calculated critical length is larger than the observed length of the PGD zone, the M. O'Rourke et al. (1995) model predicted successful the behavior of those two X-52 grade steel pipelines along Balboa Blvd. Note, however, that the procedure suggests that one of the lines (3000) is close to incipient wrinkling.

6.2.2 Tensile Failure

As indicated previously, an initial compressive failure in steel pipes subject to longitudinal PGD is more likely than an initial tensile rupture failure. That is, since the peak pipe force and strain in tension and compression are equal as shown in Figure 6.5 (Case I) and 6.6 (Case II), and the critical failure strain in compression is less, one first expects a compressive failure. One can determine the conditions for an initial tensile rupture (for example in a pipe locally reinforced in the compression region near the toe of an expected lateral spread) by substituting a tensile rupture strain into

Equation 6.3. This gives the critical length of the longitudinal PGD zone which in combination with Equation 6.4 yields the critical ground displacement. Note that the critical parameters, L_{cr} and δ_{cr} for tensile failure are larger than that for compression failure.

These values can be used to evaluate the likelihood of a subsequent tensile failure. By subsequent tensile failure, we mean a tensile rupture failure in the pipe near the head of the PGD zone, after a local buckling failure in the compression region near the toe. For Case II shown in Figure 6.6, the critical parameters can be used directly to determine the potential for a subsequent tensile rupture. In that case, L is large enough and δ is small enough so that a compression failure at Point E does not affect the state of stress in the tensile region around Point B. For Case I shown in Figure 6.5, the critical parameters for tensile failure are upper bounds for subsequent tensile failure since a compressive failure which limits the pipe force at Point D, increases the tensile force at Point B.

6.3 Influence of Expansion Joints

M. O'Rourke and Liu (1994) studied the influence of flexible expansion joints in a continuous pipeline subject to longitudinal PGD. Depending upon the location of the expansion joints, they may have no effect, have a beneficial effect or have a detrimental effect. For example, referring to Figure 6.5 (Case I) if the expansion joint is located at a distance larger than L away from the center of the PGD zone (i.e., to the left of Point A or to the right of Point E in Figure 6.5), an expansion joint would have no effect on the pipe stress and strain induced by the longitudinal PGD since the axial force in the pipe would be zero there even with no expansion joints. Similarly for Case II shown in Figure 6.6, an expansion joint to the left of Point A, to the right of Point F, or between Points C and D would have no effect.

Figures 6.7 through 6.9 illustrate the beneficial effects of two expansion joints close to the head and toe areas of a longitudinal PGD zone. In all three cases an expansion joint is located within a distance $L_1 (L_1 < L/2)$ of the head of the PGD zone (Point B) and another within $L_2 (L_2 < L/2)$ of the toe (Point E). This placement is beneficial since the peak tension and compression forces are limited to $t_u L_1$ and $t_u L_2$ respectively.

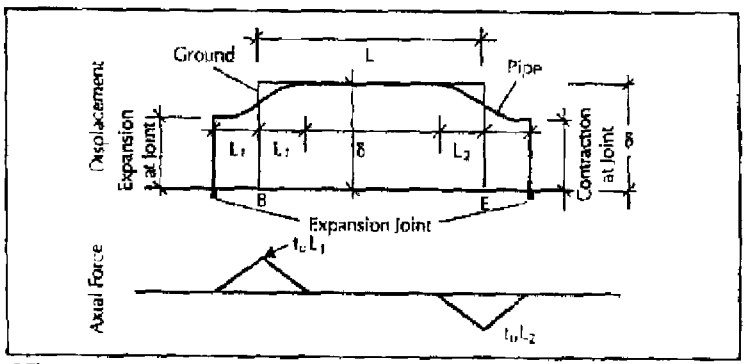

■ Figure 6.7 Pipe and Soil Displacement with Two Expansion Joints Outside PGD Zone

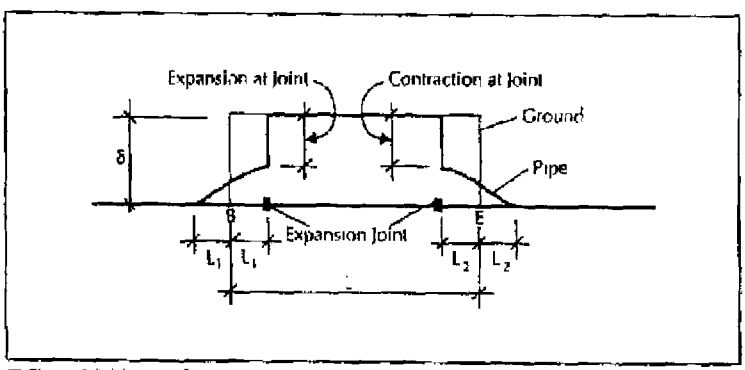

■ Figure 6.8 Pipe and Soil Displacement with Two Expansion Joints Inside PGD Zone

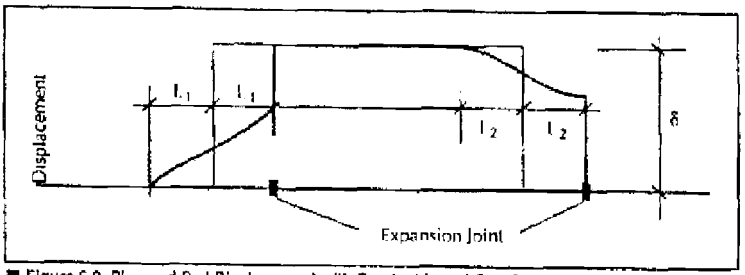

■ Figure 6.9 Pipe and Soil Displacement with One Inside and One Outside PGD Zone

Figure 6.10 illustrates the potential detrimental effects of a single expansion close to the head of a PGD zone.

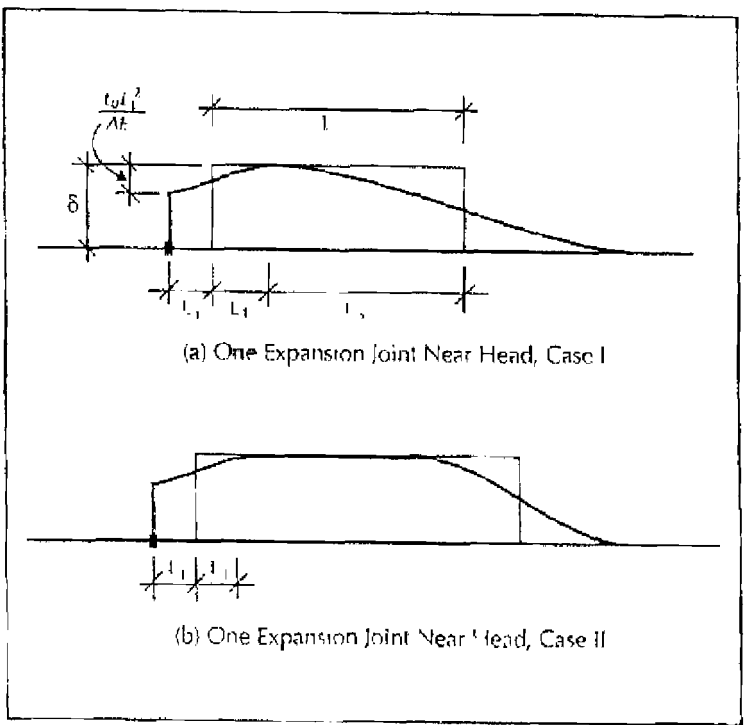

(a) One Expansion Joint Near Head, Case I

(b) One Expansion Joint Near Head, Case II

■ Figure 6.10 Pipe and Soil Displacement with a Single Expansion Joint

For Case I shown in Figure 6.10(a), the tensile stress is reduced to $t_u L_1$ but the compression stress is increased to $t_u L_2$. That is, a single expansion joint made the situation worse since the total load $t_u L$ is no longer shared equally at both the compression and tension zones. The reverse occurs for a single expansion joint near the toe region. That is for Case I the compression stress is reduced but the tensile stress increases. For Case II shown in Figure 6.10(b), the tensile stress is still reduced to $t_u L_1$ but the compression stress is unchanged.

The use of expansion joints presupposes that they are able to accommodate the imposed relative expansion and contraction. For example, if the distance L_1 and L_2 in Figure 6.9 are small (expansion joints very close to the head and toe of the PGD zone), the required expansion and contraction capability would essentially the same as the ground displacement δ. For an expansion joint at distance $L_1 (L_1 < L/2)$ away from the head or tow, the required expansion or contraction capacity is $\delta - t_u L_1^2/(AE)$ as shown in Figure 6.10.

If the amount of ground movement and required expansion/contraction capability are larger than the allowable movement of the expansion joint, the pipeline will likely be damaged. This type of damage has been observed in past events. For example, T. O'Rourke and Tawfik (1983) note that during the 1971 San Fernando earthquake, two water mains containing flexible joints were damaged at mechanical joints. However in that particular case, the pipe was subject to transverse PGD in combination of with a small amount of longitudinal PGD.

In summary, the use of expansion joints to mitigate against the effects of longitudinal PGD on continuous pipelines must be done with care. In general, to be effective, at least two expansion joints are needed, one close to the head of the PGD zone and the other close to the toe. In addition, the expansion and contraction capability of the joints themselves needs to be comparable to the amount of ground deformation δ. Finally, one needs a reasonably accurate estimate of both the location and extent of the PGD zone.

6.4 INFLUENCE OF AN ELBOW OR BEND

The response of a straight pipeline subject to longitudinal PGD is discussed in Sections 6.1 and 6.2. If an elbow or bend is located close to but beyond the margins of a longitudinal PGD zone, large pipe stresses may occur due to the induced bending moments. The case of a 90° bend in the horizontal plane is considered here. The longitudinal PGD causes the elbow to move in the direction of ground movement. This elbow movement is resisted by transverse soil springs along the transverse leg (i.e., the leg perpendicular to the direction of ground motion). The soil loading on the transverse leg results in bending moments, M, at the elbow as well as a concentrated force F (an axial force in the longitudinal leg and a corresponding shear force in the transverse leg). Similar to the models in Figures 6.5 and 6.6, two cases are considered herein as shown in Figure 6.11.

In both cases, the elbow is located at a distance L_o from the compression area (i.e., the ground movement is in a direction towards the elbow). In Case I, the length of the PGD zone, L, is small and the pipe response is controlled by the length of the PGD zone, as shown in Figure 6.11(a). In Case II, the length of the PGD zone is large and pipe response is controlled by the displacement of the PGD zone, δ, as shown in Figure 6.11(b).

In the analytical development which follows, the pipe is assumed to be elastic and the axial force per unit length along the longitudinal leg is taken as t_u. Assuming that the lateral soil spring along both the longitudinal and transverse legs are elastic, a beam on elastic foundation model of the elbow shown in Figure 6.12 results in the following relation between the imposed displacement δ' and the resulting force F:

$$\delta' = \frac{1}{2\lambda^3 EI}(F - \lambda M) \tag{6.8}$$

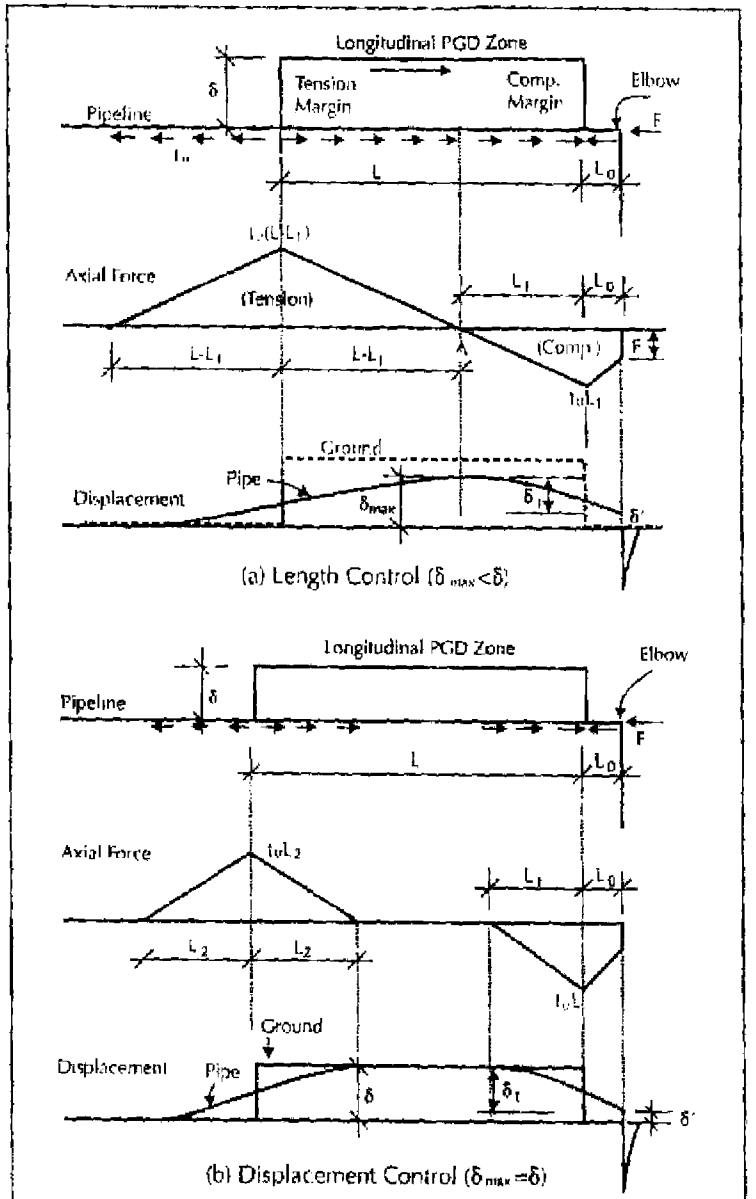

■ Figure 6.11 Pipeline with Elbow Subject to Longitudinal PGD

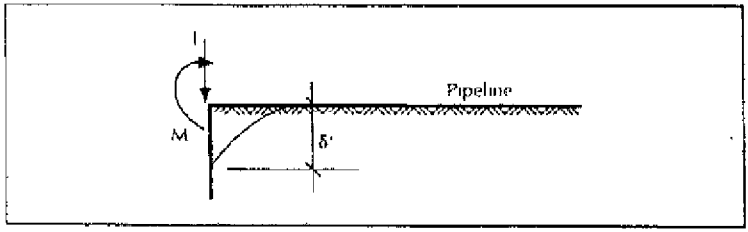

■ Figure 6.12 Model for Beam on Elastic Foundation

where,

$$\lambda = \sqrt[4]{\frac{k}{4EI}} \tag{6.9}$$

For an imposed displacement δ' at the elbow, the relation between the resulting moment and force F is given by

$$M = \frac{F}{3\lambda} \tag{6.10}$$

For a given force F at the elbow, equilibrium of the longitudinal leg near the compression margin requires:

$$F = (L_1 - L_0)t_u \tag{6.11}$$

where L_1 is the distance from the compression margin of the PGD zone to the point of zero axial pipe stress within the PGD zone (Point A in Figure 6.11(a))

For a small L case (Case I in Figure 6.11(a)), the pipe response is controlled by the length of PGD zone. The maximum pipe displacement δ_{max} is less than the ground displacement δ. Considering pipe deformation near the compression margin,

$$\delta_{max} = \delta' + \delta_1 \tag{6.12}$$

where δ' is given by Equations 6.8 and 6.10, and

$$\delta_1 = \frac{FL_0}{AE} + \frac{t_u L_0^2}{2AE} + \frac{t_u L_1^2}{2AE} \tag{6.13}$$

is the displacement due to pipe strain between Point A and the elbow.

Considering pipe deformation near the tension margin, that is integrating pipe strain to the left of Point A gives,

$$\delta_{max} = \frac{t_u(L - L_1)^2}{AE} \tag{6.14}$$

hence

$$\frac{t_u(L - L_1)^2}{AE} = \frac{F}{3EI\lambda^3} + \frac{FL_0}{AE} + \frac{t_u L_0^2}{2AE} + \frac{t_u L_1^2}{2AE} \tag{6.15}$$

For a large length case (Case II in Figure 6.11(b)), the pipe response is controlled by the maximum ground displacement. That is,

$$\delta_{max} = \delta = \delta' + \delta_1 \tag{6.16}$$

or

$$\delta = \frac{F}{3EI\lambda^3} + \frac{FL_0}{AE} + \frac{t_u L_0^2}{2AE} + \frac{t_u L_1^2}{2AE} \tag{6.17}$$

The force F at the elbow and the effective length L_1 can be obtained by simultaneously solving Equations 6.11 and 6.15 (Case I) or Equations 6.11 and 6.17 (Case II). The moment can then be calculated by Equation 6.10. When the elbow is located near the compression margin, the maximum pipe stress at the elbow is then given by:

$$\sigma = \frac{F}{A} \pm \frac{MD}{2I} \tag{6.18}$$

When the elbow is located beyond the PGD zone but close to the tension margin, the same relation applies but the force at the elbow, F, would be tension

As a case history, New Line 120 is considered herein. As shown in Figure 6.13, New Line 120 was subject to longitudinal PGD along McLennan Avenue during the 1994 Northridge earthquake. There is an elbow at about 40 m (131 ft) away from the southern (compression) margin of the PGD zone. The length of the PGD zone was about 280 m (918 ft) and the amount of ground displacement was reported to be about 0.50 m (20 in). This line is X-60 grade steel pipe with D=0.61 m (24 in), t=0.0064 m (1/4 in) and H=1.5 m (5.0 ft). For the pipe with fusion bounded epoxy coating (μ = 0.38), the axial friction force per unit length is estimated to be 1.8×10^{4} N/m (103 lbs/in) from Equation 5.1 while the lateral (transverse) spring coefficient is estimated to be 1.67×10^{6} N/m^2 (242 lbs/in^2) (1.0×10^{5} N/m (571 lbs/in) from Equation 5.5, divided by 0.06 m (2.4 in) from Equation 5.6).

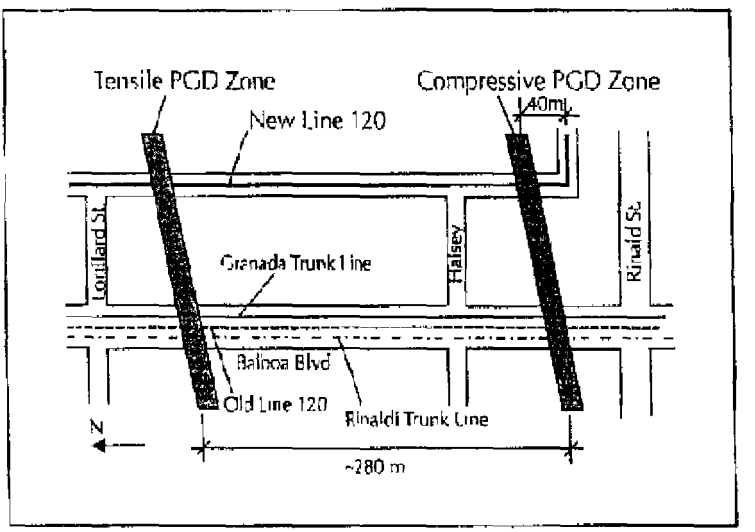

■ Figure 6.13 Observed PGD and Location of Pipeline

For Case I, Equations 6.11 and 6.15 suggest that L_1=90 m (295 ft) and Equation 6.13 gives δ_{max}=0.253 m (10 in) while for Case II Equations 6.11 and 6.17 suggest L_1=110 m (361 ft) and δ_{max}=0.50 m (20 in). Based on these parameters, the case history corresponds to Case I (i.e., length control).

For L_1=90 m (295 ft), the peak pipe stress at the compression margin $t_u L_1/A$=132 MPa (19.1 ksi), the axial stress at the elbow F/A=73 MPa (10.6 ksi) while the bending stress at the elbow M/S=1100 MPa (159 ksi). Hence, the total stress at the elbow, assuming the pipe remains elastic, is 1173 MPa (170 ksi). Note that these values, based on the analytical relation for an elastic pipe compare favorably with corresponding FE results for an elastic pipe.

Note that the results presented here are based on an elastic assumption for both the lateral soil spring coefficients and pipe material. For non-linear soil spring coefficients and elasto-plastic pipe material, the maximum stresses at the bend are less. For the New Line 120, a finite element analysis shows that the compressive stress at the compression margin is 517 MPa (75 ksi). The maximum tensile strain is 2.78×10^{-3} while the maximum compressive strain is 4.02×10^{-3} at the elbow. This compressive strain is larger than the critical strain for local buckling (1.80×10^{-3} from Equation 4.3). Hence, wrinkling is expected at the bend, but not at the compression margin.

The authors understand that the line was inspected after the Northridge event and is currently in service. No distress was noted at either the tension or compression margin. However, the elbow region was not inspected.